PROCEEDINGS OF SCIENCE

Light charged Higgs boson production at future ep colliders

O. Flores-Sánchez
Departamento de Sistemas y Computación Instituto Tecnológico de Puebla, Av. Tecnológico num. 420 Col. Maravillas, Puebla, Puebla, C.P. 72220, México.
E-mail: omar.flores@itpuebla.edu.mx

J. Hernández-Sánchez [*†]
Author affiliation
E-mail: jaime.hernandez@correo.buap.mx

C. G. Honorato
Facultad de Ciencias de la Electrónica, Benemérita Universidad Auntónoma de Puebla, Apdo. Postal 542, C.P. 72570 Puebla, Puebla, México.
E-mail: carlosg.honorato@correo.buap.mx

S. Moretti[‡]
School of Physics and Astronomy, University of Southampton, Highfield, Southampton SO17 1BJ, United Kingdom and Particle Physics Department, Rutherford Appleton Laboratory, Chilton, Didcot, Oxon OX11 0QX, United Kingdom
E-mail: s.moretti@soton.ac.uk

S. Rosado
Facultad de Ciencias Físico-Matemáticas,Benemérita Universidad Autónoma de Puebla, Apdo. Postal 1364, C.P. 72570 Puebla, Puebla, México.
E-mail: sebastian.rosado@gmail.com

We present a recent study of light charged Higgs boson (H^-) production at the Large Hadron electron Collider (LHeC). We study the charged current production process $e^- p \to \nu_e q H^-$, taking in account the decay channels $H^- \to b\bar{c}$ and $H^- \to \tau\bar{\nu}_\tau$. We analyse the process in the framework of the 2-Higgs Doublet Model Type-III (2HDM-III), assuming a four-zero texture in the Yukawa matrices and a general Higgs potential. We consider a variety of both reducible and irreducible backgrounds for the signals of the H^- state. We show that the detection of a light charged Higgs boson is feasible, assuming for the LHeC standard energy and luminosity conditions.

XXVII International Workshop on Deep-Inelastic Scattering and Related Subjects - DIS2019
8-12 April, 2019
Torino, Italy

PoS(DIS2019)094

[*] Speaker.

[†] Supported by SNI-CONACYT, VIEP-BUAP and PRODEP, México.

[‡] Supported through the NExT Institute, STFC CG grant ST/L000296/1 and H2020-MSCA-RISE-2014 grant no. 645722 (NonMinimalHiggs).

1. Introduction

After of the discovery of a neutral Higgs boson by the CMS [1] and ATLAS [2] experiments, practically, the Standard Model (SM) has been fully established. However, in several extensions of the Higgs sector Beyond the SM (BSM) which can reproduce the SM-like limit of Electro-Weak Symmetry Breaking (EWSB) using doublet Higgs fields, there appears at least one charged Higgs boson, like in the 2HDM [3]. Amongst the possible $H^{\pm}$ decay channels. the importance of the $H^{\pm} \to cb$ one has been pointed out as a possible viable signal in some models and its detection possibilities have been analysed for the LHC already several years ago [4, 5, 6, 7] and very recently for the LHeC [8, 9] as well. Our own studies have been carried out in the context of the 2HDM-III, where both Higgs doublets are coupled to both up- and down-type quarks and Flavour Changing Neutral Currents (FCNCs) can be controlled by a particular texture in the Yukawa matrices [4, 5, 10]. In this work, we present a new analysis of the signals $H^- \to b\bar{c}$ and $H^- \to \tau\bar{\nu}_\tau$ from the process $e^- p \to \nu_e q H^-$ at the LHeC machine, considering the most recent constraints from experimental data [8]. In the process $e^- p \to \nu_e q H^-$, q can be a light quark $q_l = u, d, c, s$ or a b-quark, with the production stage followed by $H^- \to b\bar{c}$ and $H^- \to \tau\bar{\nu}_\tau$ (Fig. 1), assuming a leptonic decay of the τ into an electron or muon. When the final state is $H^- \to b\bar{c}$, the main backgrounds are $\nu 3j$, $\nu 2bj$, $\nu 2jb$ and νtb (Fig. 2). For the final state $H^- \to \tau\bar{\nu}_\tau$, these are $\nu j\ell\nu$ and $\nu b\ell\nu$ (Fig. 3).

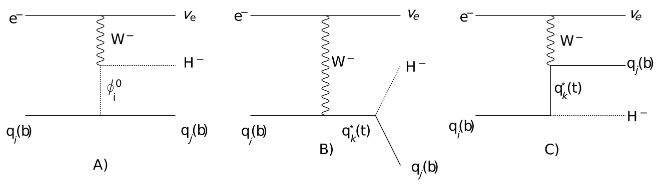

Figure 1: Feynman diagrams for the $e^-\ p \to \nu_e H^- q$ process. Here, $\phi_i^0 = h, H, A$, i.e., any of the neutral Higgs bosons of the BSM scenario considered here.

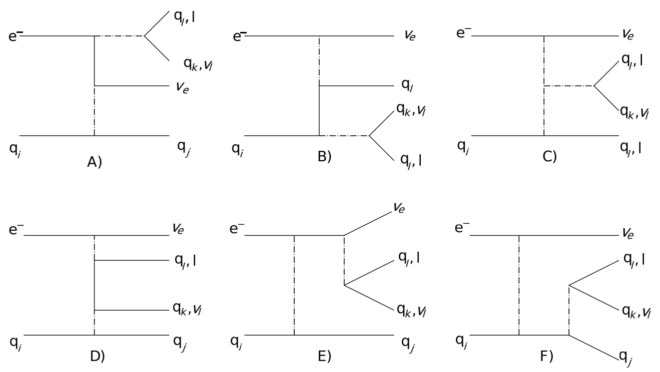

Figure 2: Feynman diagrams for the $\nu_e jjj$, $\nu_e bjj$ and $\nu_e bbj$ backgrounds (the change $q_l \leftrightarrow l$ and $q_k \leftrightarrow \nu_l$ represents the $\nu_e \nu_l lj$ and $\nu_e \nu_l lb$ backgrounds). Dash-dot lines represent boson fields: (pseudo)scalars and EW gauge bosons.

The plan of this paper is: we present the 2HDM-III in the next section, then show our results and finally conclude.

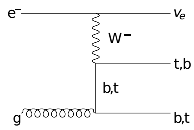

Figure 3: Feynman diagrams for the $\nu_e bt$ background.

2. 2HDM-III

For the 2HDM-III, a four-zero-texture is implemented and FCNCs are controlled. Then the most general $SU(2)_L \times U(1)_Y$ invariant scalar potential for two scalar doublets, $\Phi_i^\dagger = (\phi_i^-, \phi_i^{0*})$ ($i = 1, 2$), is considered, which is

$$\begin{aligned} V(\Phi_1,\Phi_2) \;=\; & \mu_1^2(\Phi_1^\dagger\Phi_1)+\mu_2^2(\Phi_2^\dagger\Phi_2)-\Big(\mu_{12}^2(\Phi_1^\dagger\Phi_2)+h.c.\Big)+\frac{1}{2}\lambda_1(\Phi_1^\dagger\Phi_1)^2+\frac{1}{2}\lambda_2(\Phi_2^\dagger\Phi_2)^2 \\ & +\lambda_3(\Phi_1^\dagger\Phi_1)(\Phi_2^\dagger\Phi_2)+\lambda_4(\Phi_1^\dagger\Phi_2)(\Phi_2^\dagger\Phi_1)+\Bigg[\frac{1}{2}\lambda_5(\Phi_1^\dagger\Phi_2)^2+\Big(\lambda_6(\Phi_1^\dagger\Phi_1) \\ & +\lambda_7(\Phi_2^\dagger\Phi_2)\Big)(\Phi_1^\dagger\Phi_2)+h.c.\Bigg], \end{aligned} \tag{2.1}$$

where we assume that all parameter of Higgs potential are real, including the Vacuum Expectation Values (VEVs) of the Higgs fields, $v_{1,2}$. The Yukawa Lagrangian is:

$$\mathscr{L}_Y = -\Big(Y_1^u\bar{Q}_L\tilde{\Phi}_1u_R+Y_2^u\bar{Q}_L\tilde{\Phi}_2u_R+Y_1^d\bar{Q}_L\Phi_1d_R+Y_2^d\bar{Q}_L\Phi_2d_R+Y_1^l\bar{L}\Phi_1l_R+Y_2^l\bar{L}_L\Phi_2l_R\Big), \tag{2.2}$$

where $\tilde{\Phi}_{1,2} = i\sigma_2\Phi_{1,2}^*$. The fermion mass matrices after EWSB are expressed by: $M_f = \frac{1}{2}(v_1Y_1^f + v_2Y_2^f)$, $f = u, d, l$, assuming that both Yukawa matrices Y_1 and Y_2 have the four zero-texture form and are Hermitian [4, 5, 10]. Upon diagonalising the mass matrices, one obtains the rotated matrix Y_n^f: $[\tilde{Y}_n^f]_{ij} = \frac{\sqrt{m_i^f m_j^f}}{v}[\tilde{\chi}_n^f]_{ij} = \frac{\sqrt{m_i^f m_j^f}}{v}[\chi_n^f]_{ij}e^{i\theta_{ij}^f}$, where the χ parameters can be constrained by flavour physics [5, 10], with $v = \sqrt{v_1^2+v_2^2}$. In agreement with Ref. [5], one can get a generic expression for the fermionic couplings of the charged Higgs bosons:

$$\mathscr{L}^{\bar{f}_i f_j\phi} \;=\; -\left\{\frac{\sqrt{2}}{v}\bar{u}_i(m_{d_j}X_{ij}P_R+m_{u_i}Y_{ij}P_l)d_jH^+ + \frac{\sqrt{2}m_{l_j}}{v}Z_{ij}\bar{\nu}_L l_R H^+ + h.c.\right\}, \tag{2.3}$$

where X_{ij}, Y_{ij} and Z_{ij} are defined as follows:

$$X_{ij} \;=\; \sum_{l=1}^{3}(V_{\mathrm{CKM}})_{il}\left[X\frac{m_{d_l}}{m_{d_j}}\delta_{lj}-\frac{f(X)}{\sqrt{2}}\sqrt{\frac{m_{d_l}}{m_{d_j}}}\tilde{\chi}_{lj}^d\right], \tag{2.4}$$

$$Y_{ij} \;=\; \sum_{l=1}^{3}\left[Y\delta_{il}-\frac{f(Y)}{\sqrt{2}}\sqrt{\frac{m_{u_l}}{m_{u_i}}}\tilde{\chi}_{il}^u\right](V_{\mathrm{CKM}})_{lj}, \tag{2.5}$$

$$Z_{ij}^l \;=\; \left[Z\frac{m_{l_i}}{m_{l_j}}\delta_{ij}-\frac{f(Z)}{\sqrt{2}}\sqrt{\frac{m_{l_i}}{m_{l_j}}}\tilde{\chi}_{ij}^l\right], \tag{2.6}$$

where $f(x) = \sqrt{1+x^2}$ and the parameters X, Y and Z are arbitrary complex numbers, which can be related to $\tan\beta$ or $\cot\beta$ when $\chi_{ij}^f = 0$ [5], thus one can recovers the standard four types of the 2HDM (Tab. 1)[1] and one can write the Higgs-fermion-fermion (ϕff) couplings as $g_{\mathrm{2HDM-III}}^{\phi ff} =$

[1]We will call these 2HDM-III 'incarnations' 2HDM-III like-χ scenarios, where χ = I, II, X and Y.

$g^{\phi ff}_{\text{2HDM-any}} + \Delta g$, where $g^{\phi ff}_{\text{2HDM-any}}$ is the coupling ϕff in any of the 2HDMs with discrete symmetry and Δg is the contribution of the four-zero-texture.

2HDM-III	X	Y	Z
2HDM Type I	$-\cot\beta$	$\cot\beta$	$-\cot\beta$
2HDM Type II	$\tan\beta$	$\cot\beta$	$\tan\beta$
2HDM Type X	$-\cot\beta$	$\cot\beta$	$\tan\beta$
2HDM Type Y	$\tan\beta$	$\cot\beta$	$-\cot\beta$

Table 1: The parameters X, Y and Z of the 2HDM-III defined in the Yukawa interactions when $\chi^f_{ij} = 0$ so as to recover the standard four types of 2HDM.

We take four Benchmark points (BPs) where the decay channels $H^- \to b\bar{c}$ and $H^- \to \tau\bar{\nu}_\tau$ can offer the most optimistic chances for detection [8].

- Scenario 2HDM-III like-I: $\cos(\beta-\alpha) = 0.5$, $\chi^u_{22} = 1$, $\chi^u_{23} = 0.1$, $\chi^u_{33} = 1.4$, $\chi^d_{22} = 1.8$, $\chi^d_{23} = 0.1$, $\chi^d_{33} = 1.2$, $\chi^\ell_{22} = -0.4$, $\chi^\ell_{23} = 0.1$, $\chi^\ell_{33} = 1$ with $Y \gg X, Z$.
- Scenario 2HDM-III like-II: $\cos(\beta-\alpha) = 0.1$, $\chi^u_{22} = 1$, $\chi^u_{23} = -0.53$, $\chi^u_{33} = 1.4$, $\chi^d_{22} = 1.8$, $\chi^d_{23} = 0.2$, $\chi^d_{33} = 1.3$, $\chi^\ell_{22} = -0.4$, $\chi^\ell_{23} = 0.1$, $\chi^\ell_{33} = 1$ with $X, Z \gg Y$.
- Scenario 2HDM-III like-X: the same parameters of scenario 2HDM-III like-II but $Z \gg X, Y$.
- Scenario 2HDM-III like-Y: the same parameters of scenario 2HDM-III like-II but $X \gg Y, Z$.

3. Results

We assume the LHeC standard Centre-of-Mass (CM) energy of $\sqrt{s_{ep}} \approx 1.3$ TeV and luminosity of $L = 100$ fb^{-1}. For the signatures $H^- \to b\bar{c}$ and $H^- \to \tau\nu_\tau$ the inclusive event rates are substantial, of order up to several thousands in all four cases. Some BPs, maximising the signal rates are given in Tab. 2. The scenarios and signatures that we will study are as follows.

- BPs from 2HDM-III like-I, -II and -Y, where the most relevant decay process is $H^- \to b\bar{c}$, the final state is $3j + \not{E}_T$.
- BP from 2HDM-III like-X, where the most relevant decays process is $H^- \to \tau\bar{\nu}_\tau$, the final state is $j + l + \not{E}_T$, where $l = e, \mu$ (from a leptonic τ decay) and the jet is b-tagged.

We have used CalcHEP 3.7 [11] as parton level event generator, interfaced to the CTEQ6L1 Parton Distribution Functions (PDFs) [12], then PYTHIA6 [13] for the parton shower, hadronisation and hadron decays and PGS [14] as detector emulator, by using a LHC parameter card suitably modified for the LHeC [15, 16]. We considered a calorimeter coverage $|\eta| < 5.0$, with segmentation $\Delta\eta \times \Delta\phi = 0.0359 \times 0314$. Besides, we used Gaussian energy resolution, with $\frac{\Delta E}{E} = \frac{a}{\sqrt{E}} \oplus b$, where $a = 0.085$ and $b = 0.003$ for the Electro-Magnetic (EM) calorimeter resolution and $a = 0.32$, $b = 0.086$ for the hadronic calorimeter resolution, with $\oplus$ meaning addition in quadrature [15, 16]. The algorithm to perform jet finding was a "cone" one with jet radius $\Delta R = 0.5$. The calorimeter trigger cluster finding a seed(shoulder) threshold was 5 GeV(1 GeV). We took $E_T(j) > 10$ GeV for a jet to be considered so, in addition to the isolation criterion $\Delta R(j;l) > 0.5$. Finally, we have mapped the kinematic behaviour of the final state particles using MadAnalysis5 [17].

2HDM-III	Parameters			$\sigma(ep \to \nu_e H^- q)$ (pb)				BR$(H^- \to b\bar{c})$	BR$(H^- \to \tau\bar{\nu}_\tau)$
like-	X	Y	Z	$m_{H^\pm} = 110$ GeV	130 GeV	150 GeV	170 GeV	$m_{H^\pm} = 110$ GeV	$m_{H^\pm} = 110$ GeV
I	0.5	17.5	0.5	2.56×10^{-2}	1.30×10^{-2}	3.47×10^{-3}	1.35×10^{-4}	9.57×10^{-1}	2.5×10^{-4}
II	20	1.5	20	2.18×10^{-2}	1.13×10^{-2}	2.95×10^{-3}	5.89×10^{-5}	9.9×10^{-1}	2.22×10^{-4}
X	0.03	1.5	-33.33	6.49×10^{-2}	3.39×10^{-2}	8.83×10^{-3}	2.34×10^{-4}	9.28×10^{-2}	9.04×10^{-1}
Y	13	1.5	$-1/13$	6.41×10^{-2}	3.27×10^{-2}	8.47×10^{-3}	2.2×10^{-4}	9.91×10^{-1}	6.12×10^{-3}

Table 2: The BPs that we studied for the 2HDM-III in the incarnations like-I, -II, -X and -Y. We present cross sections and *BRs* at parton level for some $H^\pm$ mass choices.

Signal	Scenario	Events (raw)	Cut I	Cut II	Cut III	Cut IV	$(\mathscr{S}/\sqrt{\mathscr{B}})_{100\,\mathrm{fb}^{-1}(1000\,\mathrm{fb}^{-1})[3000\,\mathrm{fb}^{-1}]}$
$\nu_e H^\pm b$	I-110	2562	298	182	134	54	1.43 (4.52) [7.82]
	I-130	1300	139	82	64	19	0.58 (1.82) [3.16]
	I-150	347	29	13	11	3	0.16 (0.5) [0.86]
	I-170	13	1.29	0.62	0.51	0.14	0.01 (0.03) [0.05]
$\nu_e H^\pm b$	II-110	2183	245	151	122	53	1.4 (4.43) [7.68]
	II-130	1128	128	84	71	22	0.7 (2.21) [3.82]
	II-150	294	28	14	13	4	0.2 (0.65) [1.13]
	II-170	6	0.6	0.33	0.3	0.08	0.005 (0.017) [0.029]
$\nu_e H^\pm b$	Y-110	6417	468	567	347	156	4.18 (12.99) [22.5]
	Y-130	3268	366	204	156	46	1.43 (4.53) [7.84]
	Y-150	847	68	29	23	6	0.33 (1.06) [1.83]
	Y-170	22	2.3	1.12	0.89	0.25	0.017 (0.05) [0.09]
$\nu_e bbj$		20169	2011	748	569	125	
$\nu_e bjj$		117560	10278	7211	5011	718	$\mathscr{B} = 1441$
$\nu_e bt$		41885	2278	1418	1130	188	$\sqrt{\mathscr{B}} = 37.9$
$\nu_e jjj$		867000	9238	3221	2593	409	

Table 3: Significances obtained after the sequential cuts described in the text for the signal process $e^- q \to \nu_e H^- b$ followed by $H^- \to b\bar{c}$ for four BPs in the 2HDM-III like-I, -II and -Y. The simulation is done at detector level. In the column Scenario, the label A-110(130)[150]{170} means $m_{H^\pm} = 110(130)[150]\{170\}$ GeV in the 2HDM-III like-A, where A can be I, II and Y.

3.1 The process $e^- q \to \nu_e H^- b$ with $H^- \to b\bar{c}$ for the 2HDM-III like-I, -II and -Y

In this subsection we study the final state with one b-tagged jet and one light jet (associated with the secondary decay $H^- \to b\bar{c}$).

I First, we select only events with exactly three jets in the final state. Then, we reject all events without a b-tagged jet. Then we keep events like $3j + \not{E}_T$ with at least one b-tagged jet.

II The second set of cuts is focused on selecting two jets (one b-tagged, labelled as b_{tag}, and one not, labelled as j_{c}) which are central in the detector. First, we demand that $P_T(b_{\mathrm{tag}}) > 30(40)$ GeV and $P_T(j_{\mathrm{c}}) > 20(30)$ GeV for $m_{H^\pm} = 110, 130(150, 170)$ GeV (here, P_T is the transverse momentum). Then, we impose a cut on the pseudorapidity $|\eta(b_{\mathrm{tag}}, j_{\mathrm{c}})| < 2.5$ of both these jets and, finally, select events in which $1.8(2) < \Delta R(j_{\mathrm{c}}; b_{\mathrm{tag}}) < 3.4(3.4)$ in correspondence of $m_{H^\pm} = 110, 130(150, 170)$ GeV (where ΔR is the standard cone separation).

III The next cut is related to the selection of a forward third generic jet (it can be either a light jet or a b-tagged one). Our selection for such a third jet is $|\eta| > 0.6$ (with a transverse momentum above 20 GeV).

IV We then implement the following selection criterium: $m_{H^\pm} - 20$ GeV $< M(b_{\mathrm{tag}}, j_{\mathrm{c}}) < m_{H^\pm}$. Finally, considering the presence of a hadronic $W^\pm$ boson decay, we impose that $M(j_{\mathrm{c}}, j_{\mathrm{f}}) > 80$ GeV or $M(j_{\mathrm{c}}, j_{\mathrm{f}}) < 60$ GeV (where j_{f} labels the forward jet).

PoS(DIS2019)094

Signal	Scenario	Events (raw)	Cut I	Cut II	Cut III	Cut IV	$(\mathscr{S}/\sqrt{\mathscr{B}})_{100\ \mathrm{fb}^{-1}(1000\ \mathrm{fb}^{-1})[3000\ \mathrm{fb}^{-1}]}$
$\nu_e H^- q$	X-110	6480	178	124	94	67	2.41 (7.61) [13.19]
	X-130	3390	75	54	52	35	1.13 (3.58) [6.2]
	X-150	880	6	3	2	2	0.09 (0.29) [0.5]
	X-170	20	0.4	0.3	0.2	0.09	0.01 (0.02) [0.04]
$\nu_e bbj$		20170	85	56	23	13	
$\nu_e bjj$		117559	623	340	122	84	
$\nu_e tb$		48845	460	374	149	105	$\mathscr{B} = 763$
$\nu_e jjj$		867000	981	596	267	162	$\sqrt{\mathscr{B}} = 27.62$
$\nu_e l \nu_l j$		23700	29	26	8	5	
$\nu_e l \nu_l b$		40400	1500	1203	569	392	

Table 4: Significances obtained after the sequential cuts described in the text for the signal process $e^- q \to \nu_e H^- b$ followed by $H^- \to \tau \bar{\nu}_\tau$ for four BPs in the 2HDM-III like-X. The simulation is done at detector level. In the column Scenario, the label X-110(130)[150]{170} means $m_{H^\pm} = 110(130)[150]\{170\}$ GeV in the 2HDM-III like -X.

3.2 The process $e^- q \to \nu_e H^- b$ with $H^- \to \tau \bar{\nu}_\tau$ in the 2HDM-III like-X

Now we focus our attention on the channel $H^- \to \tau \bar{\nu}_\tau$. To this effect, we look at leptonic τ decays ($\tau \to l \bar{\nu}_l \nu_\tau$, with $l = e, \mu$).

I This first set of cuts is focused on selecting events with one b-tagged jet and one lepton, by imposing $|\eta(b_{\mathrm{tag}}, l)| < 2.5$, $P_T(b_{\mathrm{tag}}, l) > 20$ GeV and the isolation condition $\Delta R(b_{\mathrm{tag}}; l) > 0.5$.

II The next set of cuts enables us to select a stiffer lepton and impose conditions on the missing transverse energy which are adapted to the trial $H^\pm$ mass. We select events with $P_T(l) > 25(40)$ GeV and $\not{E}_T > 30(40)$ GeV for $m_{H^\pm} = 110$, $130(150, 170)$ GeV.

III We impose the cut $|\eta(b_{\mathrm{tag}})| > 0.5$. Furthermore, upon defining the total hadronic transverse energy $H_T = \sum_{\mathrm{hadronic}} |P_T|$ in the final state, we select $H_T < 60$ GeV.

IV Finally, we enforce the last selection by exploiting the transverse mass $M_T(l)^2 = 2 p_T(l) \not{E}_T (1 - \cos\phi)$, where ϕ is the relative azimuthal angle between $p_T(l)$ and $\not{E}_T$, a quantity which allows one to label the candidate events reconstructing the charged Higgs boson mass. We make the following selection: $m_{H^\pm} - 50$ GeV $< M_T(l) < m_{H^\pm} + 10$ GeV.

4. Conclusions

Following the application of cuts I–IV, we obtain the signal and background rates in Tab. 3, for the 2HDM-III like-I, -II and -Y incarnations, and Tab. 4, for the like X case. Statistically, significances of the signal $\mathscr{S}$ over the cumulative background $\mathscr{B}$ are very good at low $H^\pm$ masses already for 100 fb^{-1} of luminosity. Hence, we confirm that the prospects for light H^- detection in the 2HDM-III at the LHeC are excellent.

References

[1] S. Chatchyan et. al. [CMS Colllaboration], Phys. Lett. B **716**, 30 (2012) [arXiv: 1207.7235[hep-ex]].

[2] G. Aad et. al. [ATLAS Collaboration], Phys. Lett. B **716**, 1 (2012) [arXiv:1207.7214[hep-ex]].

[3] G. C. Branco, P. M. Ferreira, L. Lavoura, M. N. Rebelo, M. Sher and J. P. Silva, Phys. Rept. **516**, 1 (2012) [arXiv:1106.0034 [hep-ph]].

[4] J. L. Diaz-Cruz, J. Hernández-Sánchez, S. Moretti, R. Noriega-Papaqui and A. Rosado, Phys. Rev. D **79**, 095025 (2009) [arXiv:0902.4490 [hep-ph]].

[5] J. Hernández-Sánchez, S. Moretti, R. Noriega-Papaqui and A. Rosado, JHEP **1307**, 044 (2013) [arXiv:1212.6818 [hep-ph]].

[6] A. G. Akeroyd *et al.*, Eur. Phys. J. C **77**, no. 5, 276 (2017) [arXiv:1607.01320 [hep-ph]].

[7] A. G. Akeroyd, S. Moretti and J. Hernández-S#anchez, Phys. Rev. D **85**, 115002 (2012) [arXiv:1203.5769 [hep-ph]].

[8] O. Flores-Sánchez, J. Hernández-Sánchez, C. G. Honorato, S. Moretti and S. Rosado-Navarro, Phys. Rev. D **99**, no. 9, 095009 (2019) [arXiv:1811.05476 [hep-ph]].

[9] J. Hernández-Sánchez, O. Flores-Sánchez, C. G. Honorato, S. Moretti and S. Rosado, PoS CHARGED **2016**, 032 (2017) [arXiv:1612.06316 [hep-ph]].

[10] O. Félix-Beltrán, F. González-Canales, J. Hernández-Sánchez, S. Moretti, R. Noriega-Papaqui and A. Rosado, Phys. Lett. B **742**, 347 (2015) [arXiv:1311.5210 [hep-ph]].

[11] A. Belyaev, N. D. Christensen and A. Pukhov, Comput. Phys. Commun. **184**, 1729 (2013) [arXiv:1207.6082 [hep-ph]].

[12] J. Pumplin, D. R. Stump, J. Huston, H. L. Lai, P. M. Nadolsky and W. K. Tung, JHEP **0207**, 012 (2002) [hep-ph/0201195].

[13] T. Sjostrand, S. Mrenna and P. Z. Skands, JHEP **0605**, 026 (2006) [hep-ph/0603175].

[14] J. Conway, R. Culbertson, R. Demina, B. Kilminster, M. Kruse, S. Mrenna, J. Nielsen, M. Roco, A. Pierce, J. Thaler and T. Wizansky, http://conway.physics.ucdavis.edu/research/software/pgs/pgs4-general.htm.

[15] J. L. Abelleira Fernandez *et al.* [LHeC Study Group], J. Phys. G **39**, 075001 (2012) [arXiv:1206.2913 [physics.acc-ph]].

[16] O. Bruening and M. Klein, Mod. Phys. Lett. A **28**, no. 16, 1330011 (2013) [arXiv:1305.2090 [physics.acc-ph]].

[17] E. Conte, B. Fuks and G. Serret, Comput. Phys. Commun. **184**, 222 (2013) [arXiv:1206.1599 [hep-ph]].